Histone demethylase JMJD2C is a coactivator for hypoxia-inducible factor 1 that is required for breast cancer progression

Weibo Luo[a,b], Ryan Chang[a], Jun Zhong[b], Akhilesh Pandey[b,c,d,e], and Gregg L. Semenza[a,b,c,e,f,g,h,1]

[a]Vascular Program, Institute for Cell Engineering, Departments of [b]Biological Chemistry, [c]Oncology, [d]Pathology, [f]Pediatrics, [g]Medicine, and [h]Radiation Oncology, and [e]McKusick–Nathans Institute of Genetic Medicine, The Johns Hopkins University School of Medicine, Baltimore, MD 21205

Contributed by Gregg L. Semenza, October 5, 2012 (sent for review July 24, 2012)

Hypoxia-inducible factor 1 (HIF-1) activates transcription of genes encoding proteins that play key roles in breast cancer biology. We hypothesized that interaction of HIF-1 with epigenetic regulators may increase HIF-1 transcriptional activity, and thereby promote breast cancer progression. We report that the histone demethylase jumonji domain containing protein 2C (JMJD2C) selectively interacts with HIF-1α, but not HIF-2α, and that HIF-1α mediates recruitment of JMJD2C to the hypoxia response elements of HIF-1 target genes. JMJD2C decreases trimethylation of histone H3 at lysine 9, and enhances HIF-1 binding to hypoxia response elements, thereby activating transcription of *BNIP3*, *LDHA*, *PDK1*, and *SLC2A1*, which encode proteins that are required for metabolic reprogramming, as well as *LOXL2* and *L1CAM*, which encode proteins that are required for lung metastasis. JMJD2C expression is significantly associated with expression of GLUT1, LDHA, PDK1, LOX, LOXL2, and L1CAM mRNA in human breast cancer biopsies. JMJD2C knockdown inhibits breast tumor growth and spontaneous metastasis to the lungs of mice following mammary fat pad injection. Taken together, these findings establish an important epigenetic mechanism that stimulates HIF-1–mediated transactivation of genes encoding proteins involved in metabolic reprogramming and lung metastasis in breast cancer.

H3K9me3 | SILAC | chromatin immunoprecipitation | gene expression

Maintenance of oxygen homeostasis underlies many developmental and physiological processes, and disturbances of oxygen homeostasis play key roles in the pathogenesis of many human diseases, including cancer, diabetes, and ischemic cardiovascular disease (1). Hypoxia-inducible factors (HIFs) regulate adaptive responses to reduced O_2 availability in all metazoan species and play essential roles in embryonic development, postnatal physiology, and disease pathogenesis (2–7). HIFs are heterodimeric transcription factors, consisting of α and β subunits (8). Three α subunits (HIF-1α, HIF-2α, and HIF-3α) and one β subunit (HIF-1β) have been identified (8–12). In well-oxygenated cells, HIF-α subunits are hydroxylated on proline residues by prolyl hydroxylases (PHDs) in the presence of reaction substrates (O_2 and α-ketoglutarate) and cofactors (iron and ascorbate) (13). The von Hippel–Lindau tumor suppressor protein binds to prolyl hydroxylated HIF-α subunits and promotes their ubiquitination and degradation in the 26*S* proteasome (14). Under hypoxic conditions, PHD activity is inhibited (13). As a result, HIF-α proteins are stabilized and translocate to the nucleus. HIF-1α (or HIF-2α) dimerizes with HIF-1β, and the heterodimer binds to DNA at sites containing the consensus nucleotide sequence 5′-RCGTG-3′ within the hypoxia response element (HRE) of target genes to activate transcription (15). More than 1,000 genes have been identified as HIF target genes, many of which are transactivated by both HIF-1 and HIF-2 (1, 16). However, HIF-1 and HIF-2 each also controls a battery of unique target genes. The amino-terminal transactivation domains (TADs) of the HIF-α subunits may determine the specificity of target genes transactivated by HIF-1 or HIF-2 (17).

A growing number of proteins have been shown to regulate HIF transcriptional activity. Factor inhibiting HIF-1 negatively regulates the transcriptional activity of HIFs in nonhypoxic cells (18) by catalyzing the asparaginyl hydroxylation of HIF-1α (or HIF-2α), which blocks the recruitment of the coactivator p300 to the carboxyl-terminal TAD of HIF-α (19). In hypoxic cells, the histone acetyltransferase p300 catalyzes the acetylation of lysine residues on the amino-terminal tail of core histones to induce changes in chromatin structure, which facilitates the transcription of HIF target genes (20). Histone deacetylase (HDAC) 7 interacts with HIF-1α and p300 to increase HIF-1 transcriptional activity (21). HDAC4 induces deacetylation of HIF-1α to increase HIF-1–mediated transactivation (22). The class III HDAC sirtuin 1 deacetylates HIF-2α in hypoxic cells to stimulate HIF-2–mediated transactivation (23), whereas it inhibits HIF-1 activity by deacetylating HIF-1α at lysine 674 (24). Histone lysine methylation is also involved in HIF-1–mediated transactivation. The histone demethylase jumonji domain (JMJD) containing protein 1A demethylates dimethylated lysine 9 of histone H3 (H3K9me2) and enhances transcription of the HIF-1 target genes *SLC2A3* and *KDM3A* (25). The ATP-dependent chromatin remodeling factors Pontin and Reptin regulate HIF-1 transcriptional activity as well (26, 27). Pontin interacts with HIF-1α to enhance transcription of the HIF-1 target gene *ETS1*, thereby promoting migration of MCF-7 breast cancer cells (26). Methylation of Pontin by the histone methyltransferases G9a and GLP is required for coactivator function. In contrast, Reptin is methylated by G9a and represses HIF-1–dependent transcription in cancer cells (27).

HIFs are activated in many solid tumors as a result of intratumoral hypoxia and/or genetic alterations (4, 16). Proteins encoded by HIF target genes are involved in critical steps of cancer progression, including angiogenesis, glucose and energy metabolism, and cell survival and proliferation, as well as invasion and metastasis (28, 29). For example, LOX family members mediate ECM remodeling and metastatic niche formation (30–32). L1CAM mediates interaction of breast cancer cells with vascular endothelial cells to promote cancer cell extravasation (33). The histone demethylase JMJD containing protein 2C (JMJD2C), which is encoded by the *KDM4C* gene, is an HIF-1 target gene (34). JMJD2C specifically demethylates trimethylated lysine 9 of histone H3 (H3K9me3), H3K9me2, trimethylated lysine 36 of histone H3 (H3K36me3), and H3K36me2 in vitro and in cells overexpressing JMJD2C (35, 36). JMJD2C cooperates with lysine-specific demethylase 1 and activates androgen re-

Author contributions: W.L. and G.L.S. designed research; W.L., R.C., and J.Z. performed research; W.L., J.Z., A.P., and G.L.S. analyzed data; and W.L. and G.L.S. wrote the paper.

The authors declare no conflict of interest.

[1]To whom correspondence should be addressed. E-mail: gsemenza@jhmi.edu.

See Author Summary on page 19889 (volume 109, number 49).

This article contains supporting information online at www.pnas.org/lookup/suppl/doi:10.1073/pnas.1217394109/-/DCSupplemental.

ceptor-mediated gene expression in LNCaP human prostate cancer cells by decreasing H3K9me3 at the promoter of the androgen receptor target genes *PSA* and *KLK2* (37). The *KDM4C* gene is located in a region of chromosome 9p24 that is amplified in various human cancers, including breast cancer (38, 39). JMJD2C levels are significantly higher in aggressive basal-like breast cancer than in non–basal-like breast cancer (40). Although JMJD2C promotes cancer cell transformation and proliferation (40), the potential roles of JMJD2C in HIF activation and breast cancer metastasis have not been investigated.

In the present study, we demonstrate that JMJD2C functions as a coactivator for HIF-1 and stimulates HIF-1–mediated transactivation in cancer cells. JMJD2C decreases H3K9me3 at the HREs of HIF-1 target genes and enhances HIF-1 binding to HREs, thereby promoting gene transcription. Knockdown of JMJD2C inhibits breast tumor growth and lung metastasis in mice. The physical and functional interaction of JMJD2C with HIF-1α represents a critical epigenetic mechanism underlying HIF-1–mediated transactivation of genes encoding the lethal metastatic phenotype in breast cancer.

Results

JMJD2C Interacts Selectively with HIF-1α. To identify proteins that selectively regulate the transcriptional activity of HIF-1 or HIF-2, we screened for HIF-1α– and HIF-2α–interacting proteins in HeLa human cervical carcinoma cells treated with the PHD inhibitor dimethyloxalylglycine (DMOG) for 24 h, using GST fusion proteins containing the TAD of HIF-1α (residues 531–826) or HIF-2α (residues 450–870) as bait in a quantitative stable isotope labeling by amino acids in cell culture (SILAC) proteomic assay (Fig. 1*A*). HeLa cells were chosen for analysis because they express both HIF-1α and HIF-2α, and are therefore an appropriate cell type in which to study regulators of either HIF-1 or HIF-2. Mass spectrometry (MS) identified 44 hits with a ratio of heavy peaks to light peaks ≥2 and a ratio of medium peaks to light peaks <2 as selective HIF-1α–interacting proteins, 42 hits with a ratio of medium peaks to light peaks ≥2 and a ratio of heavy peaks to light peaks <2 as selective HIF-2α–interacting proteins, and 146 hits with a ratio of heavy and medium peaks to light peaks ≥2 as HIF-1α– and HIF-2α–interacting proteins (Fig. 1*B*). JMJD2C was chosen for further analysis because of its known role as a histone demethylase. JMJD2C peptides were detected in GST–HIF-1α (residues 531–826) precipitates only, but not in GST or GST–HIF-2α (residues 450–870) precipitates (Fig. 1*C*), thereby identifying JMJD2C as a protein that selectively interacts with HIF-1α in vitro.

To confirm the proteomic finding, we performed a coimmunoprecipitation (co-IP) assay. HeLa cells were exposed to 1% O_2 for 24 h, and nuclear lysates were subjected to co-IP assays. Endogenous HIF-1α, but not HIF-2α, was specifically precipitated from nuclear lysates by anti-JMJD2C antibody, but not by control IgG (Fig. 2*A*). No specific HIF-2α band was detected in JMJD2C immunoprecipitates from whole-cell lysates of hypoxic HeLa cells that overexpressed exogenous HIF-2α (Fig. S1). Conversely, using anti–HIF-1α antibody, endogenous JMJD2C was coimmunoprecipitated from hypoxic HeLa whole-cell lysates (Fig. 2*B*). These data indicate that endogenous JMJD2C physically interacts with HIF-1α, but not HIF-2α, in human cancer cells.

The proteomic data presented above demonstrated that JMJD2C bound to GST–HIF-1α (residues 531–826) (Fig. 1*C*), encoding the HIF-1α TAD (41), which was verified by in vitro GST pull-down assays (Fig. 2*C*). JMJD2C failed to interact with GST fusion proteins containing residues 1–80, 81–200, 201–329, 331–427, or 432–528 of HIF-1α (Fig. 2*C*). Fine mapping of the subdomain within the TAD that binds to JMJD2C revealed that JMJD2C bound to GST–HIF-1α (residues 575–786), but not to GST, GST–HIF-1α (residues 531–588), or GST–HIF-1α (residues 786–826) (Fig. 2*D*).

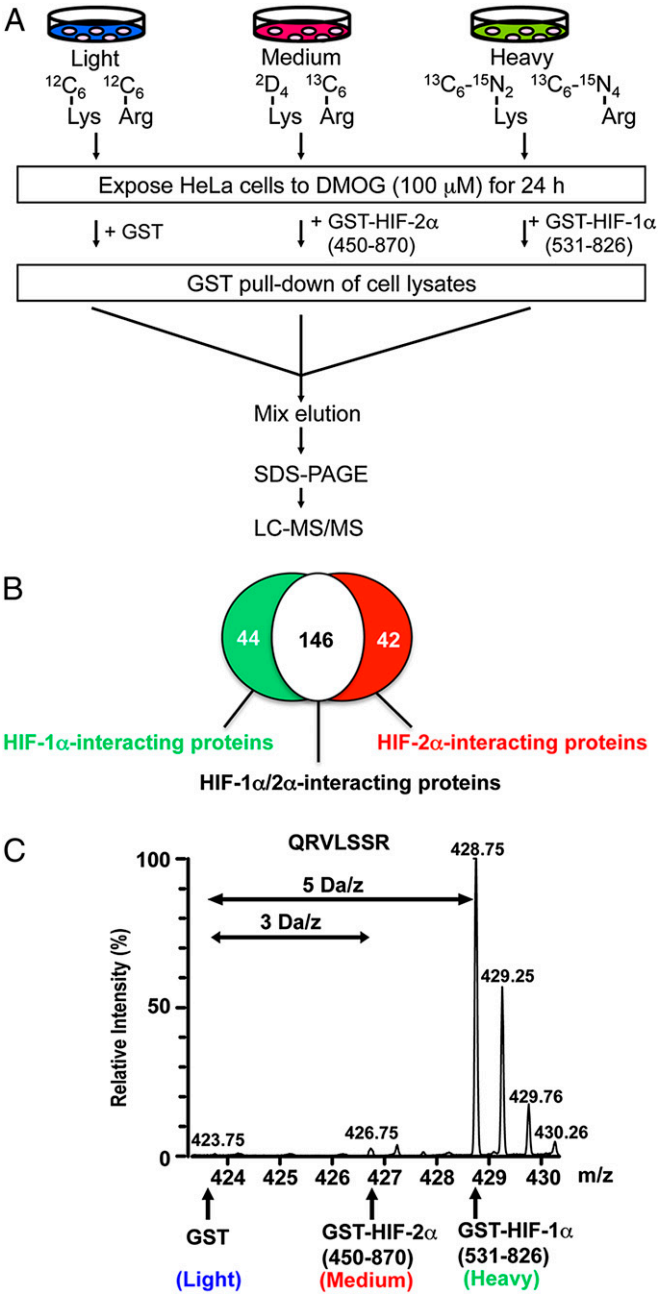

Fig. 1. JMJD2C is an HIF-1α–interacting protein. (*A*) Stable isotope labeling by amino acids in cell culture (SILAC) proteomic screen was performed to identify HIF-1α– and HIF-2α–interacting proteins. (*B*) Number of HIF-1α– and/or HIF-2α–interacting proteins pulled down by GST fusion proteins in the SILAC screen is shown. (*C*) Mass spectrum of a JMJD2C tryptic peptide is shown. Monoisotopic peaks derived from JMJD2C bound to GST–HIF-2α (residues 450–870) and GST–HIF-1α (residues 531–826) are 3 Da/z and 5 Da/z greater, respectively, than peaks derived from JMJD2C bound to GST.

We also determined the JMJD2C domain that binds to HIF-1α by GST pull-down assays. GST-JMJD2C fusion proteins were purified from bacteria and incubated with lysates from HeLa cells exposed to 1% O_2 for 4 h to induce HIF-1α stabilization. HIF-1α interacted strongly with GST-JMJD2C (residues 144–310), which encodes the catalytic domain of JMJD2C (36), but not with GST or GST fusion proteins containing other domains of JMJD2C (Fig. 2*E*).

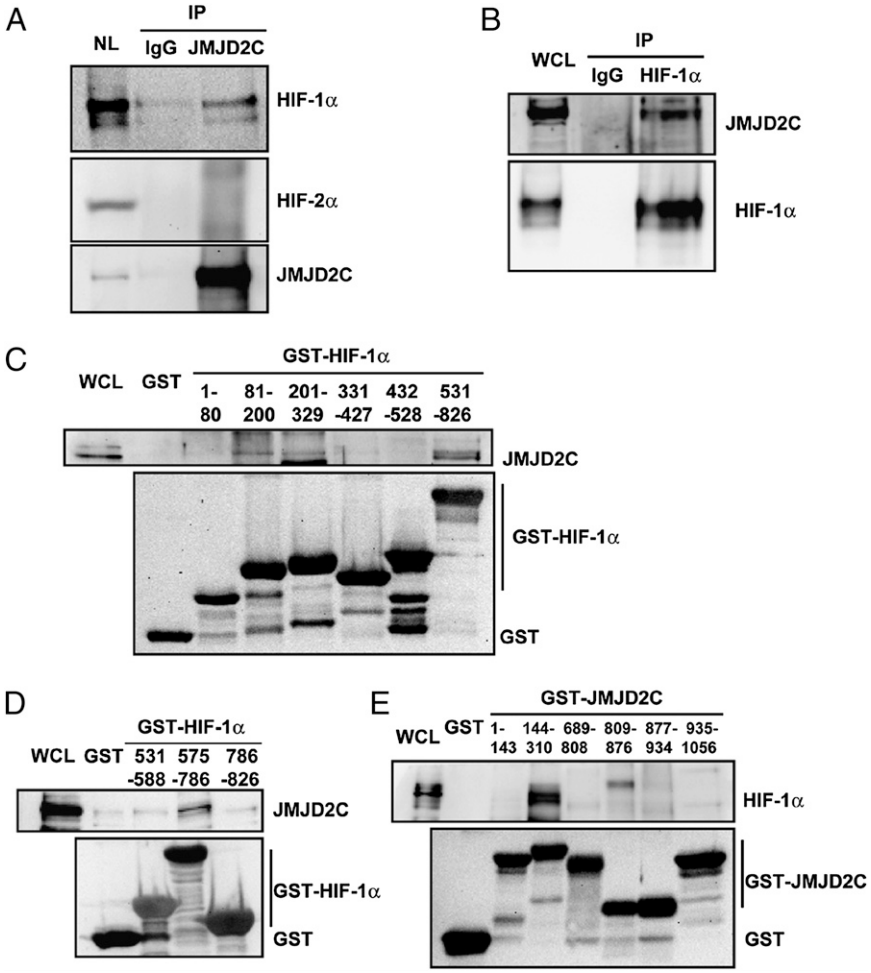

Fig. 2. JMJD2C interacts with HIF-1α in vitro and in human cancer cells. (*A*) Co-IP was performed using anti-JMJD2C antibody or IgG control and nuclear lysate (NL) from HeLa cells exposed to 1% O_2 for 24 h. (*B*) Co-IP was performed using anti–HIF-1α or IgG control and whole-cell lysate (WCL) from HeLa cells exposed to 1% O_2 for 24 h. (*C* and *D*) GST pull-down assays were performed with GST or GST fusion protein containing the indicated amino acid residues of HIF-1α and WCL from HeLa cells exposed to 1% O_2 for 24 h. (*E*) GST pull-down assays were performed with GST or GST fusion protein containing the indicated residues of JMJD2C and WCL from HeLa cells exposed to 1% O_2 for 4 h.

JMJD2C Stimulates HIF-1–Mediated Transcription. To test whether JMJD2C regulates HIF-1 transcriptional activity, HeLa cells were cotransfected with the following: HIF-1–dependent reporter plasmid p2.1, which contains an HRE from the human *ENO1* gene upstream of SV40 promoter and firefly luciferase coding sequences (15); control reporter pSV-Renilla; and empty vector (EV) or expression vector encoding either V5 epitope-tagged JMJD2C or FLAG epitope-tagged HIF-1α. The ratio of p2.1/pSV-Renilla activity is a specific measure of HIF-1 transcriptional activity. Expression of FLAG–HIF-1α dramatically increased HIF-1 transcriptional activity, which was further enhanced by coexpression of JMJD2C-V5 (Fig. 3*A*). However, JMJD2C-V5 coexpression failed to increase HIF-2 transcriptional activity in nonhypoxic HeLa cells with forced expression of HIF-2α (Fig. 3*B*). To complement the gain-of-function studies, we also performed loss-of-function studies by transfection of a vector encoding shRNA directed against JMJD2C (shJMJD2C) or a scrambled control shRNA (shSC). Knockdown of endogenous JMJD2C expression by either of two independent shJMJD2Cs (shJMJD2C-1 or shJMJD2C-2) significantly reduced HIF-1 transcriptional activity compared with shSC in hypoxic HeLa cells (Fig. 3*C* and Fig. S2*A*). HIF-1α protein levels were not affected by either JMJD2C overexpression or JMJD2C knockdown (Fig. 4 *B* and *C* and Fig. S3*A*). Taken together, these data indicate that JMJD2C specifically stimulates the transcriptional activity of HIF-1, but not HIF-2, in HeLa cells.

We further studied the direct effect of JMJD2C on HIF-1α TAD function. HeLa cells were cotransfected with the following: expression vector pGalA, which encodes the GAL4 DNA-binding domain fused to the HIF-1α TAD (residues 531–826); reporter plasmid pG5E1bLuc, which contains five GAL4-binding sites and a TATA box upstream of firefly luciferase coding sequences (41); pSV-Renilla; and shSC or shJMJD2C expression vector. The transfected cells were exposed to 20% or 1% O_2 for 24 h. Hypoxia increased GalA-dependent transcriptional activity in HeLa cells transfected with vector encoding shSC, whereas GalA-dependent transcription was significantly reduced by transfection of shJMJD2C-1 or shJMJD2C-2 vector (Fig. 3*D* and Fig. S2*B*). These data indicate that JMJD2C directly stimulates HIF-1α TAD function.

To determine whether the histone demethylase activity of JMJD2C is required to stimulate HIF-1α transactivation, we generated an expression vector encoding a triple-mutant JMJD2C (JMJD2C-TM), in which three key residues in the catalytic center of the enzyme (His-190, Glu-192, and His-278) were mutated to Ala. Immunoblot data showed that overexpression of wild-type (WT) JMJD2C-V5 (JMJD2C-WT) reduced levels of H3K9me3, whereas JMJD2C-TM failed to do so (Fig. S3*B*), confirming the

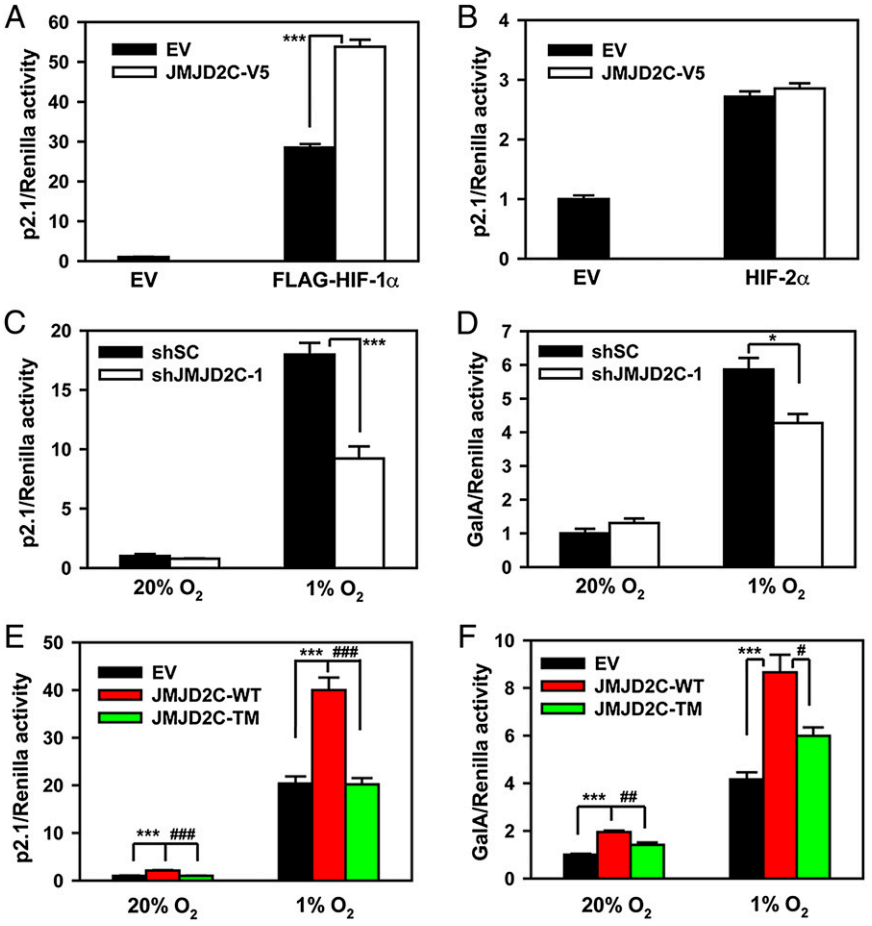

Fig. 3. JMJD2C stimulates HIF-1–dependent transactivation. (*A* and *B*) HeLa cells were transfected with HIF-1–dependent firefly luciferase (FLuc) reporter p2.1, control Renilla luciferase (RLuc) reporter pSV-Renilla, and one or more of the following expression vectors, as indicated: empty vector (EV), JMJD2C-V5, FLAG–HIF-1α, or HIF-2α for 24 h. The ratio of FLuc/RLuc activity was normalized to EV (mean ± SEM, $n = 4$). ***$P < 0.001$. (*C* and *E*) HeLa cells were transfected with p2.1, pSV-Renilla, and expression vector encoding shRNA targeting JMJD2C (shJMJD2C) or scrambled shRNA (shSC) (*C*), or expression vector encoding JMJD2C-WT or JMJD2C-TM (*E*) and were exposed to 20% or 1% O_2 for 24 h. The FLuc/RLuc ratio was normalized to shSC (*C*) or EV (*E*) at 20% O_2 (mean ± SEM, $n = 4$). ***$P < 0.001$; ###$P < 0.001$. (*D* and *F*) HeLa cells were transfected with expression vector pGalA, FLuc reporter pG5E1bLuc, pSV-Renilla, and the indicated expression vector and were exposed to 20% or 1% O_2 for 24 h. The FLuc/RLuc ratio was normalized to shSC (*D*) or EV (*F*) at 20% O_2 (mean ± SEM, $n = 4$). *$P < 0.05$; ***$P < 0.001$; #$P < 0.05$; ##$P < 0.01$.

loss of catalytic activity of JMJD2C-TM. It was demonstrated by means of p2.1 and pGalA reporter assays that JMJD2C-WT, but not JMJD2C-TM, significantly increased HIF-1 transactivation in HeLa cells (Fig. 3 *E–F*). These data indicate that the histone demethylase activity of JMJD2C is required for stimulation of HIF-1 transcriptional activity.

JMJD2C Stimulates HIF-1 Target Gene Expression. To determine whether JMJD2C regulates expression of HIF-1 target genes involved in cancer progression, MDA-MB-435 human breast cancer cells were transduced with retroviruses expressing shJMJD2C-1 and shJMJD2C-2 or with retrovirus expressing shSC. The transduced cells were exposed to 20% or 1% O_2 for 24 h. JMJD2C knockdown significantly decreased expression of the HIF-1 target genes *LDHA*, *PDK1*, *LOXL2*, and *L1CAM* in hypoxic MDA-MB-435 cells (Fig. 4*A*). In contrast, JMJD2C knockdown failed to inhibit transcription of the HIF-2 target gene *CITED2* in MDA-MB-435 cells (Fig. 4*A*). We also observed significantly reduced expression of the HIF-1 target genes *LDHA*, *PDK1*, *SLC2A1* (which encodes GLUT1), and *BNIP3*, but not of the non–HIF-1 target gene *RPL13A* (Fig. S4*A*), in hypoxic HeLa cells transduced with lentivirus carrying tetracycline-inducible (Tet-on)–shJMJD2C-1 in the presence of doxycycline, which resulted in decreased JMJD2C protein levels (Fig. S4*B*). Expression of the HIF-2 target gene *SOD2* was significantly induced by hypoxia, but SOD2 mRNA levels were not decreased in JMJD2C knockdown HeLa cells (Fig. S4*A*). LDHA, PDK1, and GLUT1 protein levels were significantly reduced in JMJD2C knockdown MDA-MB-435 cells exposed to 1% O_2 (Fig. 4 *B* and *C*). The JMJD2C shRNAs had greater inhibitory effects on JMJD2C protein than on JMJD2C mRNA levels, suggesting that they repressed mRNA translation. Taken together, the data presented in Figs. 3 and 4 demonstrate that JMJD2C selectively coactivates HIF-1 target genes in human breast and cervical cancer cells.

JMJD2C Enhances HIF-1 Binding to HREs. To determine whether JMJD2C binds to the HREs of HIF-1 target genes, HeLa cells were exposed to 20% or 1% O_2 for 24 h. ChIP assays demonstrated significantly increased occupancy by JMJD2C of HREs at the HIF-1 target genes *LDHA* and *PDK1* in hypoxic compared with nonhypoxic HeLa cells (Fig. 5*A* and Fig. S5*A*). However, hypoxia did not increase HRE occupancy by other members of the JMJD2 family, including JMJD containing protein 2A (JMJD2A) and JMJD containing protein 2D (JMJD2D) (Fig. S6). We next determined the role of HIF-1α in recruitment of JMJD2C to the HREs of HIF-1 target genes. Transduction of lentivirus encoding an HIF-1α shRNA (shHIF-1α) effectively

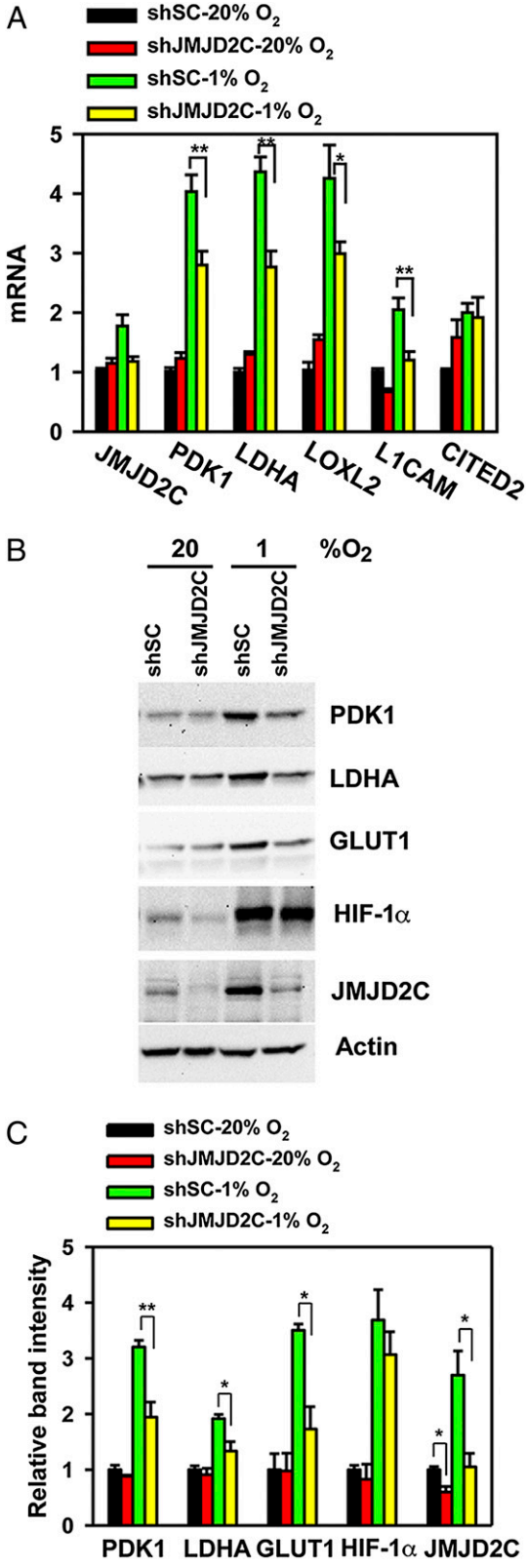

Fig. 4. JMJD2C increases expression of HIF-1 target genes. MDA-MB-435 cells were cotransduced with retroviruses encoding shJMJD2C-1 and shJMJD2C-2 or with retrovirus encoding shSC and were exposed to 20% or 1% O_2 for 24 h. (*A*) Quantitative real-time RT-PCR analyses of the indicated mRNAs were performed (mean ± SEM, $n = 3$). $^*P < 0.05$; $^{**}P < 0.01$. (*B*) Immunoblot assays of the indicated proteins were performed. (*C*) Band intensity was quantified and normalized to actin (mean ± SEM, $n = 4$). $^*P < 0.05$; $^{**}P < 0.01$.

knocked down HIF-1α protein levels in HeLa cells exposed to 20% or 1% O_2 for 24 h (Fig. S7). JMJD2C occupancy at the HREs of the *LDHA* and *PDK1* genes was significantly reduced in hypoxic HeLa–shHIF-1α cells compared with HeLa-shSC cells (Fig. 5*A* and Fig. S5*A*). In contrast, HIF-1α knockdown failed to alter JMJD2C occupancy at the non–HIF-1 target gene *RPL13A* (Fig. S5*B*). Therefore, HIF-1 mediates recruitment of JMJD2C specifically to HIF-1 target genes in hypoxic cells.

To determine whether JMJD2C regulates levels of H3K9me3 and H3K36me3 at the HREs of HIF-1 target genes, HeLa–Tet-on–shJMJD2C-1 cells were cultured with or without doxycycline at 20% or 1% O_2 for 24 h. JMJD2C knockdown significantly increased levels of H3K9me3 at the HREs of the *LDHA* (Fig. 5*B*) and *PDK1* (Fig. S8*A*) genes in hypoxic HeLa cells. H3K36me3 levels were not altered at the *LDHA* (Fig. 5*B*) or *PDK1* (Fig. S8*A*) HRE but were significantly increased at the *RPL13A* gene (Fig. S8*B*) in doxycycline-treated Tet-on–shJMJD2C-1 cells exposed to 1% O_2 for 24 h. Levels of total histone H3 at the *LDHA* and *PDK1* HREs and at the *RPL13A* gene were not affected by JMJD2C knockdown in HeLa cells (Fig. 5*B* and Fig. S8 *A* and *B*). JMJD2C knockdown also failed to alter the global levels of H3K9me3 or H3K36me3, or total histone H3 levels, in HeLa cells exposed to 20% or 1% O_2 for 24 h (Fig. S8*C*). Therefore, JMJD2C selectively demethylates H3K9me3 at the HREs of the HIF-1 target genes *LDHA* and *PDK1* but demethylates both H3K9me3 and H3K36me3 at the non–HIF-1 target gene *RPL13A*.

We next investigated effects of JMJD2C on the binding of HIF-1 to DNA in HeLa–Tet-on–shJMJD2C-1 cells exposed to 20% or 1% O_2 for 24 h in the presence or absence of doxycycline. As expected, hypoxia markedly increased HIF-1α occupancy at the *LDHA* HRE (Fig. 5*C*). JMJD2C knockdown significantly decreased HIF-1α binding to the *LDHA* HRE in doxycycline-treated Tet-on–shJMJD2C-1 cells exposed to 1% O_2 for 24 h (Fig. 5*C*). Overexpression of JMJD2C-WT significantly increased HIF-1α binding to the *LDHA* HRE (Fig. S9*A*). JMJD2C-TM failed to increase HIF-1α occupancy at the *LDHA* HRE (Fig. S9*A*). Similar to HIF-1α occupancy, HIF-1β occupancy at the *LDHA* and *PDK1* HREs was significantly inhibited by JMJD2C knockdown in doxycycline-treated Tet-on–shJMJD2C-1 cells (Fig. 5*D* and Fig. S10*A*). JMJD2C overexpression or knockdown did not affect HIF-1α or HIF-1β binding to *RPL13A* (Figs. S9*B* and S10 *B* and *C*). HIF-1α and HIF-1β protein levels were not altered by doxycycline treatment (Fig. S4*B*). Inhibitory effects of JMJD2C knockdown on HIF-1 occupancy at the *LDHA* and *PDK1* HREs were also observed in hypoxic MDA-MB-435 cells transduced with lentivirus encoding Tet-on–shJMJD2C-1 or retroviruses encoding shJMJD2C-1 and shJMJD2C-2 (Fig. S10 *D*–*H*). These data indicate that JMJD2C enhances HIF-1 binding to the HREs of target genes, which is dependent on its demethylase activity, thereby promoting HIF-1 transactivation.

JMJD2C Stimulates Breast Tumor Growth and Metastasis in Mice. To determine whether JMJD2C promotes breast tumor growth in vivo, MDA-MB-435 cells transduced with Tet-on–shJMJD2C-2 or Tet-on–shSC vector were orthotopically implanted into the mammary fat pad of SCID mice, which received drinking water with or without doxycycline. Doxycycline significantly reduced primary breast tumor growth in mice bearing Tet-on–shJMJD2C-2 cells but had no effects on tumor growth in mice bearing Tet-on–shSC cells (Fig. 6*A*). Immunoblot assays demonstrated that JMJD2C protein levels were reduced in primary breast tumors harvested from doxycycline-exposed mice implanted with Tet-on–shJMJD2C-2 cells, compared with tumors from mice bearing Tet-on–shJMJD2C-2 cells that were not exposed to doxycycline or with tumors from mice bearing Tet-on–shSC cells with or without doxycycline (Fig. 6*B*). These data indicate that JMJD2C knockdown impairs the growth of primary breast tumors in mice.

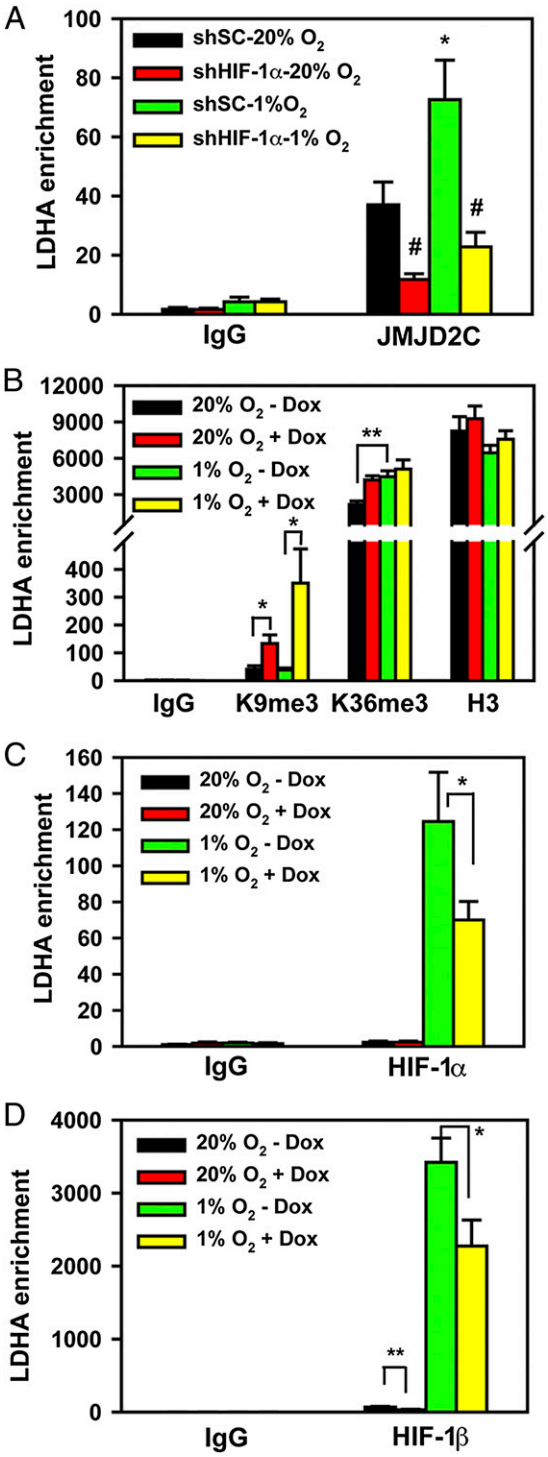

Fig. 5. JMJD2C decreases H3K9me3 and increases HIF-1 binding to the HREs of the target genes. (*A*) HeLa cells were transduced with lentivirus encoding shSC or shHIF-1α and exposed to 20% or 1% O_2 for 24 h. Chromatin was precipitated with IgG or anti-JMJD2C antibody and was analyzed by quantitative PCR with primers spanning the *LDHA* HRE (mean ± SEM, $n = 4$). $^{\#}P < 0.05$ vs. shSC; $^{*}P < 0.05$ vs. shSC-20% O_2. (*B–D*) HeLa–Tet-on–shJMJD2C-1 cells were treated with (+) or without (–) doxycycline (Dox) for 48 h and exposed to 20% or 1% O_2 for 24 h. Chromatin was precipitated with IgG control antibody, antihistone H3K9me3 antibody, antihistone H3K36me3, and antihistone H3 antibody (*B*), anti–HIF-1α antibody (*C*), or anti–HIF-1β antibody (*D*) and was analyzed by quantitative PCR with primers spanning the *LDHA* HRE (mean ± SEM, $n = 3–6$). $^{*}P < 0.05$; $^{**}P < 0.01$.

We next determined whether JMJD2C promotes the spontaneous metastasis of breast cancer cells to the lungs. H&E staining detected abundant metastases in the lungs of mice 8 wk after mammary fat pad injection of Tet-on–shSC cells (Fig. 6 *C* and *D*). Extensive metastatic disease was also detected in the lungs of mice bearing Tet-on–shJMJD2C-2 cells that were not exposed to doxycycline (Fig. 6 *C* and *D*). However, only rare and very small tumor foci were found in the lungs of doxycycline-exposed mice bearing Tet-on–shJMJD2C-2 cells (Fig. 6 *C* and *D*). Analysis of human genomic DNA in the lungs by quantitative real-time PCR also demonstrated that doxycycline significantly reduced the number of human breast cancer cells in the lungs of mice implanted with Tet-on–shJMJD2C-2 cells, but not in the lungs of mice implanted with Tet-on–shSC cells (Fig. 6*E*). Thus, JMJD2C knockdown dramatically impairs the metastasis of breast cancer cells in mice.

JMJD2C Is Highly Expressed in Human Breast Cancers. We used mRNA microarray data in the Oncomine database (Compendia Bioscience) (42, 43) to analyze JMJD2C expression in normal human breast tissues and breast cancer biopsies. JMJD2C mRNA levels were significantly increased in invasive ductal breast carcinomas and lobular breast carcinomas, compared with normal breast (Fig. 7*A*). Stromal cells play important roles in primary tumor growth and progression (44). Increased expression of JMJD2C mRNA was also observed in invasive breast carcinoma stroma, compared with normal breast (Fig. 7*B*). Moreover, JMJD2C mRNA expression in stromal cells was significantly correlated with tumor grade in patients with breast cancer (Fig. 7*C*). We further analyzed the association between JMJD2C mRNA expression and expression of HIF-1 target genes in human breast carcinoma and found that expression of GLUT1, LDHA, PDK1, LOX, LOXL2, and L1CAM mRNA was significantly increased in human invasive ductal breast carcinomas and lobular breast carcinomas (Fig. 7*D*) that highly expressed JMJD2C mRNA (Fig. 7*A*). In contrast, expression of the HIF-2 target gene *CITED2* in invasive ductal breast carcinoma and lobular breast carcinoma was comparable to that in normal breast tissues (Fig. 7*D*). Thus, JMJD2C is highly expressed in human breast cancer, and increased expression of JMJD2C is associated with elevated tumor grade and increased expression of HIF-1 target genes in human breast cancers.

Discussion

In the present study, we have demonstrated that JMJD2C selectively interacts with HIF-1α and functions as an HIF-1–specific coactivator to stimulate transcription of the *SLC2A1*, *LDHA*, and *PDK1* genes by decreasing H3K9me3 levels and increasing HIF-1 occupancy at the HREs of target genes. Increased JMJD2C expression was also significantly associated with increased expression of GLUT1, PDK1, and LDHA mRNA in human breast cancer biopsies. Increased HIF-1–dependent expression of GLUT1 enhances glucose uptake, PDK1 inactivates pyruvate dehydrogenase and shunts pyruvate away from the mitochondria, and LDHA catalyzes the conversion of pyruvate to lactate (45). Our findings therefore suggest that increased expression of JMJD2C stimulates the reprogramming of glucose metabolism in breast cancer cells. Glycolytic metabolism is used to generate macromolecular building blocks (nucleotides, amino acids, and acetyl CoA) for cancer cell proliferation (46) and to protect hypoxic cells from oxidant injury (45). Thus, JMJD2C stimulates HIF-1–dependent glucose reprogramming, which, in turn, may facilitate breast tumor growth and metastasis. JMJD2C has also been shown to coactivate androgen receptor-dependent gene expression (37), and further analysis is required to study the global effects of JMJD2C on gene transcription in cancer.

Cancer cell dissemination from the primary tumor to distant organs involves several biological steps (47), which are under the

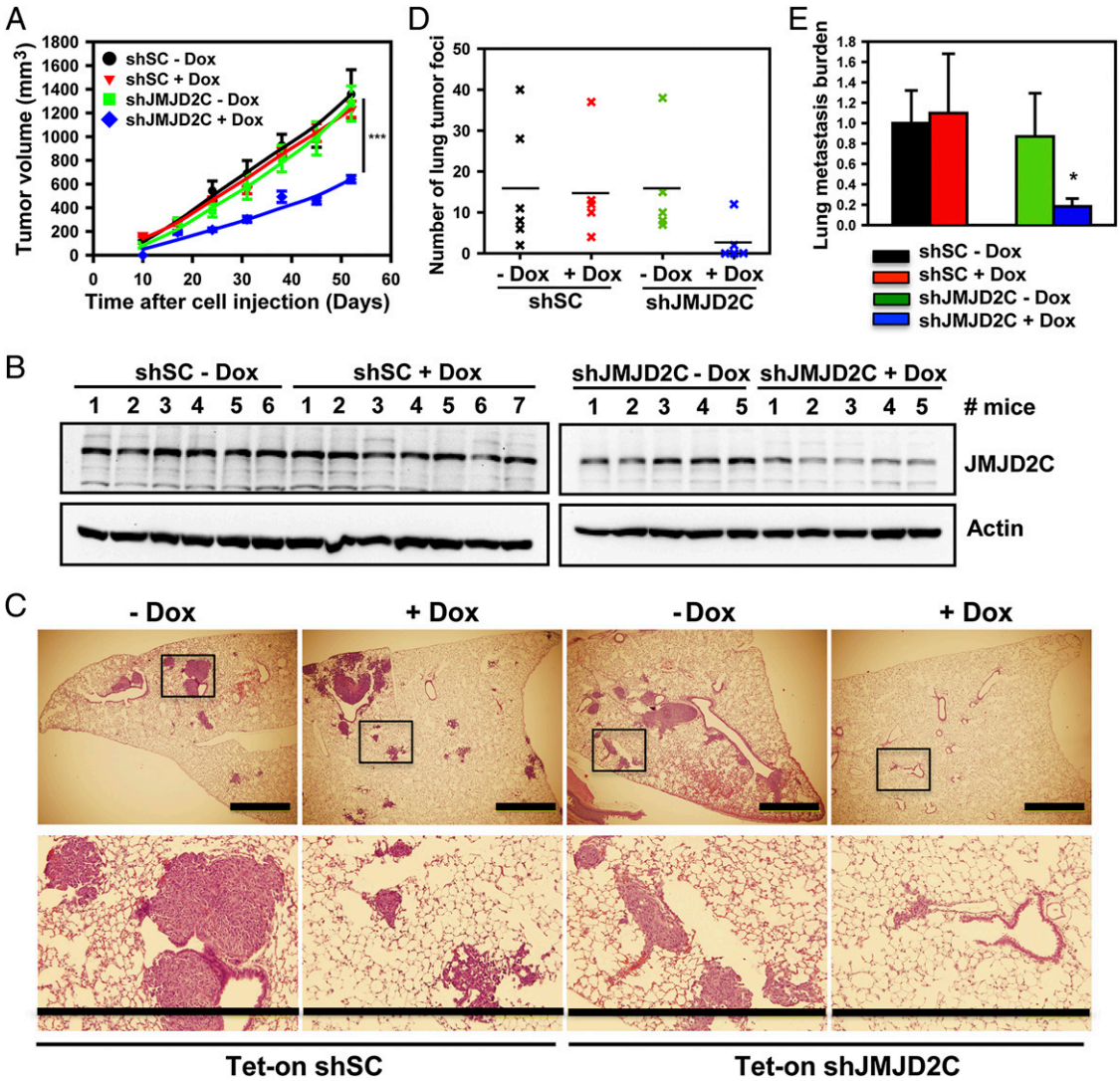

Fig. 6. JMJD2C promotes breast tumor growth and lung metastasis. MDA-MB-435–Tet-on–shSC and MDA-MB-435–Tet-on–shJMJD2C cells were treated with (+Dox) or without (–Dox) doxycycline for 48 h and implanted into the mammary fat pad of SCID mice (n = 5–7). (*A*) Primary tumor volume was determined from day 10 to day 52 (mean ± SEM). ***$P < 0.001$. (*B*) JMJD2C and actin levels in the primary tumor were determined by immunoblot assays. (*C*) Metastases in the left lung were analyzed by H&E staining. (*Lower*) Magnified images of the boxed areas are shown. (Scale bar = 1 mm.) (*D*) Number of metastatic foci in the lungs per mouse is shown (mean ± SEM). (*E*) Genomic DNA was purified from the right lung and analyzed by quantitative PCR with human-specific *HK2* primers and 18S rRNA primers that recognized both human and mouse 18S rRNA. The ratio of the ΔCt value of HK2 /18S rRNA was normalized to the results for shSC –Dox (mean ± SEM). *$P < 0.05$ vs. –Dox.

control of proteins encoded by HIF-1 target genes. For example, LOXL2 mediates ECM remodeling and metastatic niche formation (30, 31), whereas L1CAM mediates the interaction of breast cancer cells with vascular endothelial cells to promote cancer cell margination and extravasation (33). JMJD2C coactivated expression of the HIF-1 target genes *LOXL2* and *L1CAM* in breast cancer cells, indicating that JMJD2C amplifies HIF-1–dependent expression of genes encoding proteins that mediate multiple steps required for breast cancer metastasis. Future studies are needed to study to what extent the effect of JMJD2C on breast cancer growth and metastasis is HIF-1–dependent.

Based on the histological appearance of cancer cells in biopsy sections, breast cancers are classified as grade 1 (well-differentiated), grade 2 (moderately differentiated), or grade 3 (poorly differentiated). Advanced tumor grade (i.e., grade 2 or 3) is a major risk factor for lung metastasis in patients with breast cancer (48), and JMJD2C mRNA levels were significantly increased in grade 2 and 3 breast cancers. JMJD2C also functioned as a coactivator for HIF-1 in HeLa cells, and further studies are required to determine whether JMJD2C plays critical roles in the metastasis of cervical cancers.

Histone demethylases remove methyl groups from lysine residues of histone tails, and by doing so, they modulate gene transcription (49). Our findings have elucidated the role of the histone demethylase JMJD2C in HIF-1–mediated transactivation in cancer cells. JMJD2C preferentially demethylated H3K9me3 at the HREs of the HIF-1 target genes *LDHA* and *PDK1* but had no effect on H3K36me3 levels at these sites. Occupancy of HIF-1 at the HREs may interfere with JMJD2C binding to H3K36me3, because HIF-1α interacts with the catalytic domain of JMJD2C. In contrast, JMJD2C demethylated both H3K9me3 and H3K36me3 at the non–HIF-1 target gene *RPL13A*. H3K9me3 is enriched in pericentromeric heterochromatin and is associated with gene repression (50). Demethylation of H3K9me3 induces changes in chromatin structure and increases binding of transcription factors to DNA, thereby stimulating gene transcription. Therefore, in-

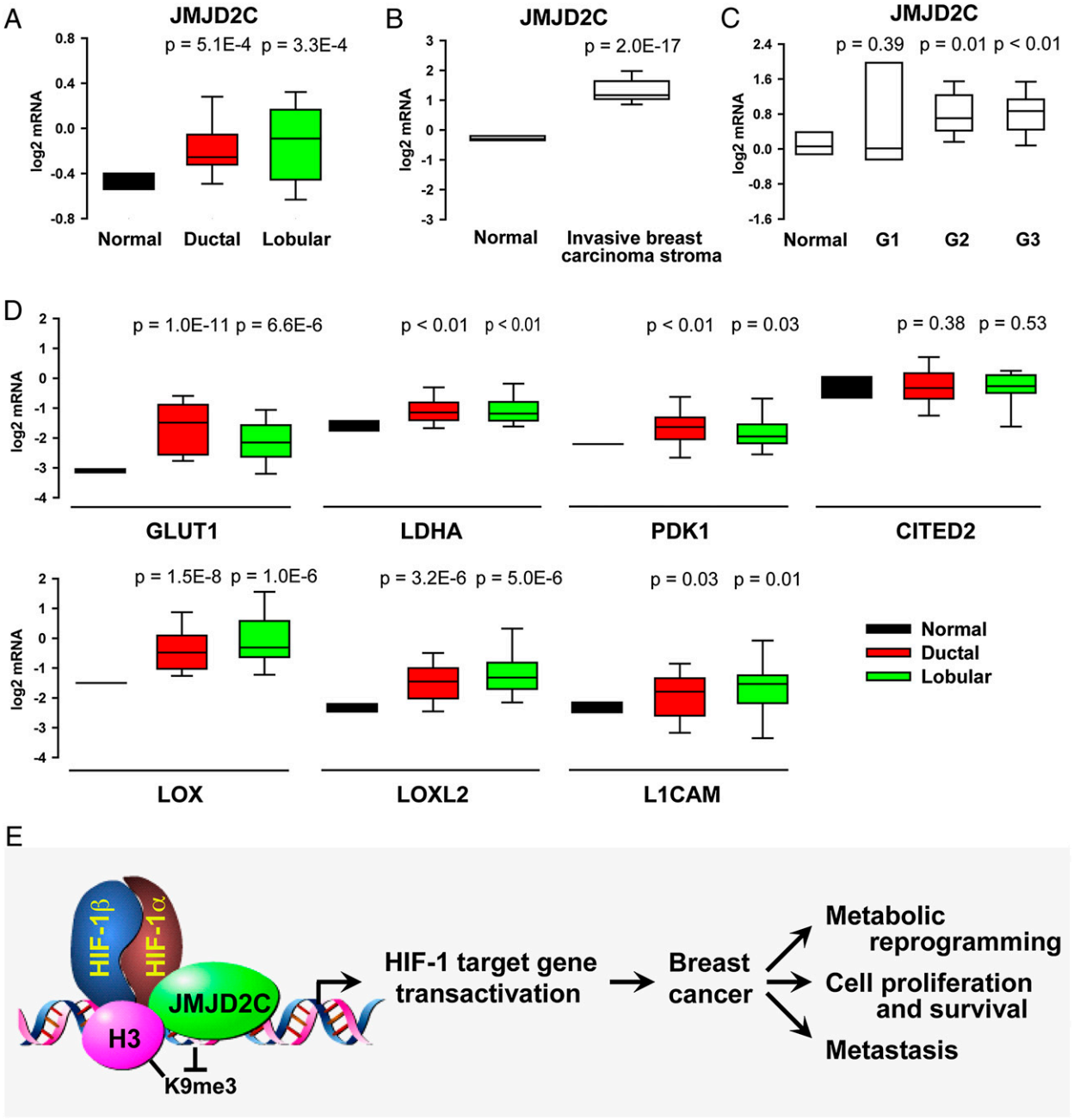

Fig. 7. JMJD2C mRNA expression is increased in human breast cancer and associated with HIF-1 target gene expression. Expression of JMJD2C (*A*), GLUT1 (*D*), LDHA (*D*), PDK1 (*D*), LOX (*D*), LOXL2 (*D*), L1CAM (*D*), and CITED2 (*D*) mRNA in normal breast tissues (n = 3); invasive ductal breast carcinoma (n = 38); and lobular breast carcinoma (n = 21). (*B*) JMJD2C mRNA expression in normal breast tissues (n = 6) and invasive breast carcinoma stroma (n = 53). (*C*) JMJD2C mRNA expression in normal breast tissues (n = 6) and in grade 1 (G1; n = 3), grade 2 (G2; n = 23), and grade 3 (G3; n = 27) breast carcinoma stroma. All mRNA expression data were obtained from the Oncomine database (42, 43). (*E*) JMJD2C demethylates H3K9me3 to increase HIF-1 binding to the HRE of the target genes and stimulates transcription of HIF-1 target genes, thereby promoting breast cancer growth and lung metastasis.

teraction of JMJD2C with HIF-1α enhances the binding of HIF-1 to HREs by decreasing H3K9me3, thereby providing a positive feedback mechanism that amplifies HIF-1–mediated transactivation in cancer cells. In contrast, H3K36me3 is present in actively transcribed regions, and demethylation of H3K36me3 inhibits gene transcription (51). Thus, there is no net effect of JMJD2C on *RPL13A* transcription. JMJD2C has been shown to demethylate nonhistone proteins (52), and future studies are required to determine whether JMJD2C demethylates HIF-1α or other proteins in the HIF-1 transcriptional complex.

The intratumoral microenvironment of human breast cancers is characterized by regions of hypoxia with median PO_2 values of 10 mmHg (~1.5% O_2), compared with 65 mmHg in normal breast (53). Intratumoral hypoxia leads to increased HIF-1α levels in the primary tumor, which is associated with increased risk of metastasis and patient mortality (54). We found that hypoxia increased the binding of JMJD2C to the HREs of HIF-1 target genes, and recruitment of JMJD2C was associated with increased HIF-1 occupancy, leading to enhanced transcription of HIF-1 target genes. JMJD2C is highly expressed in human breast

cancer biopsies, which, in part, reflects transcriptional activation of *KDM4C* by HIF-1 within regions of intratumoral hypoxia. JMJD2C-mediated H3K9 demethylation represents an important epigenetic mechanism underlying increased HIF-1–mediated transactivation in human breast cancers. The catalytic site of JMJD2C may be susceptible to inhibition by competitive antagonists of α-ketoglutarate (55), and JMJD2C may therefore represent a novel target for breast cancer therapy.

Materials and Methods

Plasmid Constructs. The complete coding sequence of human JMJD2C was amplified from HEK293 cell cDNA by PCR and inserted into pcDNA3.1D-V5-His-TOPO vector (Invitrogen). The cDNAs encoding JMJD2C domains were amplified by PCR and subcloned in pGex-6P-1 (GE Healthcare). Catalytically inactive JMJD2C (H190A/E192A/H278A) was generated using a QuikChange Site-Directed Mutagenesis Kit (Stratagene). The shRNA oligonucleotides targeting JMJD2C (Table S1) were annealed and ligated into *Bgl*II/HindIII-linearized pSUPER.retro.neo.GFP retroviral vector (OligoEngine) or *Age*I/EcoRI-linearized Tet-on–pLKO lentiviral vector (56). Other constructs have been described previously (57, 58). Plasmid constructs were confirmed by nucleotide sequencing.

Cell Culture and Transfection. HeLa, HEK293T, and MDA-MB-435 cells were cultured in DMEM with 10% heat-inactivated FBS at 37 °C in a 5% CO_2/95% air incubator. To subject cells to hypoxia, they were placed in a modular incubator chamber (Billups–Rothenberg) and flushed with a gas mixture containing 1% O_2, 5% CO_2, and 94% N_2. Cells were transfected using PolyJet (SignaGen) according to the manufacturer's protocol. Cells expressing Tet-on–shJMJD2C-1 or Tet-on–shJMJD2C-2 were treated with doxycycline (0.5 μg/mL) for 48 h before experiments.

Virus Production. Retrovirus or lentivirus was generated by transfection of HEK293T cells with transducing vector and packaging vectors pMD.G and pNGVL3-gag/pol (for retrovirus) or pCMVR8.91 (for lentivirus). After 48 h, virus particles in the medium were harvested, filtered, and transduced into HeLa or MDA-MB-435 cells.

Stable Isotope Labeling by Amino Acids in Cell Culture Assays. HeLa cells were cultured in DMEM supplemented with high glucose (4.5 g/L), 10% FBS, and $^{12}C_6$-$^{14}N_2$-lysine/$^{12}C_6$-$^{14}N_4$-arginine ("light"), $^{2}D_4$-lysine/$^{13}C_6$-$^{14}N_4$-arginine ("medium"), or $^{13}C_6$-$^{15}N_2$-lysine/$^{13}C_6$-$^{15}N_4$-arginine ("heavy") for at least six population doublings and were treated with the PHD inhibitor DMOG (100 μM) for 24 h to induce HIF transcriptional activity, which facilitates detection of those HIF-α–interacting proteins (e.g., JMJD2C) that are products of HIF target genes. One hundred milligrams of whole-cell lysates from light, medium, or heavy HeLa cells was incubated overnight with GST, GST–HIF-2α (residues 470–870) or GST–HIF-1α (residues 531–826), respectively, immobilized on glutathione-Sepharose beads. The bound proteins were eluted, mixed, and fractionated by SDS/PAGE and were visualized by staining with Colloidal Blue (Invitrogen). Stained protein bands were excised and digested with trypsin. After in-gel digestion, the resulting tryptic peptides were extracted, dried, and reconstituted in 0.1% formic acid. The peptide mixture was analyzed by liquid chromatography-tandem MS (MS/MS). MS spectra were acquired on a quadrupole time-of-flight mass spectrometer (Micromass Q-TOF US-API; Water Corp.) in a survey scan (*m/z* range: 350–1,200) in a data-dependent mode, selecting the four most abundant ions for MS/MS fragmentation (*m/z* range: 100–1,800). The acquired data were processed, searched against the National Center for Biotechnology Information Protein database (March 5, 2007), and quantified using Mascot Distiller software (version 2.3.2.0; Matrix Science).

GST Pull-Down Assays. GST fusion proteins were expressed in *Escherichia coli* BL21-Gold (DE3) and purified. Mammalian cells were lysed in radioimmunoprecipitation assay buffer, and nuclear lysates were prepared using hypotonic buffer (57). Co-IP, GST pull-down, and immunoblot assays were performed as described (57, 58).

Luciferase Reporter Assays. Cells were seeded onto 48-well plates and transfected with the following: reporter plasmid p2.1 (15) or reporter plasmid pG5E1bLuc and pGalA or pGalO (41); reporter pSV-Renilla; and expression vector encoding JMJD2C-WT, JMJD2C-TM, shSC, or shJMJD2C. Transfected cells were exposed to 20% or 1% O_2 for 24 h. Firefly luciferase and Renilla luciferase activities in cell lysates were determined using the Dual-Luciferase Assay System (Promega).

Quantitative RT-PCR Assays. Total RNA was isolated using TRIzol (Invitrogen), and quantitative RT-PCR assays were performed as described (57). Primer sequences are listed in Table S1.

ChIP Assays. Cells were exposed to 20% or 1% O_2 for 24 h, cross-linked with 1% formaldehyde for 20 min at 37 °C, and quenched in 0.125 M glycine. DNA was immunoprecipitated from the sonicated cell lysates and quantified by SYBR Green real-time PCR (Bio-Rad) (57). The following antibodies were used: HIF-1α (Santa Cruz Biotechnology); HIF-1β, JMJD2A, JMJD2C, JMJD2D, and histone H3 (Novus Biologicals); and H3K9me3 and H3K36me3 (Abcam). Fold enrichment was calculated based on the cycle threshold (Ct) as $2^{-\Delta(\Delta Ct)}$, where $\Delta Ct = Ct_{IP} - Ct_{Input}$ and $\Delta(\Delta Ct) = \Delta Ct_{antibody} - \Delta Ct_{IgG}$.

Orthotopic Transplantation Assays. Animal studies were approved by the Johns Hopkins University Animal Care and Use Committee in accordance with the National Institutes of Health Guide for the Care and Use of Laboratory Animals. MDA-MB-435 cells were trypsinized and resuspended at 1.5×10^7 cells/mL in PBS/Matrigel (1:1; BD Biosciences), and 1.5×10^6 cells were implanted into the second left mammary fat pad of female SCID mice (5–7 wk old). Mice were given access to water or water supplemented with 1 mg/mL doxycycline. Primary tumor volume was measured with digital calipers and calculated as length (mm) × [width (mm)]^2 × 0.52. On day 52 after implantation, primary tumors were harvested and analyzed by immunoblot assays. Lungs were perfused with PBS. The left lung was inflated with 0.5% agarose, fixed in formalin, and embedded in paraffin, and sections were analyzed by H&E staining. Genomic DNA was isolated from the right lung and analyzed by quantitative PCR with primers for human *HK2* and mouse and human 18S rRNA genes.

Statistical Analysis. Data were expressed as mean ± SEM. Differences were analyzed by the Student *t* test for two groups and by ANOVA for multiple groups. $P < 0.05$ was considered significant.

ACKNOWLEDGMENTS. We thank Karen Padgett (Novus Biologicals) for providing antibodies against HIF-1β, HIF-2α, JMJD2A, JMJD2C, JMJD2D, GLUT1, PDK1, LDHA, histone H3, and rabbit IgG and Carmen Wong for advice on the orthotopic mouse model of breast cancer. This work was supported by National Heart, Lung, and Blood Institute Contracts N01-HV28180 and HHS-N268201000032C and by funds from the Johns Hopkins Institute for Cell Engineering. W.L. was supported by a fellowship from the Fowler Foundation for Advanced Research in the Medical Sciences. G.L.S. is the C. Michael Armstrong Professor at The Johns Hopkins University School of Medicine and an American Cancer Society Research Professor.

1. Semenza GL (2010) Oxygen homeostasis. *Wiley Interdiscip Rev Syst Biol Med* 2(3): 336–361.
2. Nangaku M, Eckardt KU (2007) Hypoxia and the HIF system in kidney disease. *J Mol Med (Berl)* 85(12):1325–1330.
3. Semenza GL (2007) Life with oxygen. *Science* 318(5847):62–64.
4. Brahimi-Horn MC, Chiche J, Pouysségur J (2007) Hypoxia and cancer. *J Mol Med (Berl)* 85(12):1301–1307.
5. Shohet RV, Garcia JA (2007) Keeping the engine primed: HIF factors as key regulators of cardiac metabolism and angiogenesis during ischemia. *J Mol Med (Berl)* 85(12):1309–1315.
6. Taylor CT, Colgan SP (2007) Hypoxia and gastrointestinal disease. *J Mol Med (Berl)* 85(12):1295–1300.
7. Zinkernagel AS, Johnson RS, Nizet V (2007) Hypoxia inducible factor (HIF) function in innate immunity and infection. *J Mol Med (Berl)* 85(12):1339–1346.
8. Wang GL, Jiang BH, Rue EA, Semenza GL (1995) Hypoxia-inducible factor 1 is a basic-helix-loop-helix-PAS heterodimer regulated by cellular O_2 tension. *Proc Natl Acad Sci USA* 92(12):5510–5514.
9. Semenza GL, Wang GL (1992) A nuclear factor induced by hypoxia via de novo protein synthesis binds to the human erythropoietin gene enhancer at a site required for transcriptional activation. *Mol Cell Biol* 12(12):5447–5454.
10. Ema M, et al. (1997) A novel bHLH-PAS factor with close sequence similarity to hypoxia-inducible factor 1α regulates the VEGF expression and is potentially involved in lung and vascular development. *Proc Natl Acad Sci USA* 94(9):4273–4278.
11. Gu YZ, Moran SM, Hogenesch JB, Wartman L, Bradfield CA (1998) Molecular characterization and chromosomal localization of a third alpha-class hypoxia inducible factor subunit, HIF3alpha. *Gene Expr* 7(3):205–213.
12. Tian H, McKnight SL, Russell DW (1997) Endothelial PAS domain protein 1 (EPAS1), a transcription factor selectively expressed in endothelial cells. *Genes Dev* 11(1): 72–82.
13. Kaelin WG, Jr., Ratcliffe PJ (2008) Oxygen sensing by metazoans: The central role of the HIF hydroxylase pathway. *Mol Cell* 30(4):393–402.
14. Maxwell PH, et al. (1999) The tumour suppressor protein VHL targets hypoxia-inducible factors for oxygen-dependent proteolysis. *Nature* 399(6733):271–275.

15. Semenza GL, et al. (1996) Hypoxia response elements in the aldolase A, enolase 1, and lactate dehydrogenase A gene promoters contain essential binding sites for hypoxia-inducible factor 1. *J Biol Chem* 271(51):32529–32537.
16. Semenza GL (2012) Hypoxia-inducible factors in physiology and medicine. *Cell* 148(3): 399–408.
17. Hu CJ, Sataur A, Wang L, Chen H, Simon MC (2007) The N-terminal transactivation domain confers target gene specificity of hypoxia-inducible factors HIF-1α and HIF-2α. *Mol Biol Cell* 18(11):4528–4542.
18. Mahon PC, Hirota K, Semenza GL (2001) FIH-1: A novel protein that interacts with HIF-1α and VHL to mediate repression of HIF-1 transcriptional activity. *Genes Dev* 15(20): 2675–2686.
19. Lando D, Peet DJ, Whelan DA, Gorman JJ, Whitelaw ML (2002) Asparagine hydroxylation of the HIF transactivation domain a hypoxic switch. *Science* 295(5556): 858–861.
20. Arany Z, et al. (1996) An essential role for p300/CBP in the cellular response to hypoxia. *Proc Natl Acad Sci USA* 93(23):12969–12973.
21. Kato H, Tamamizu-Kato S, Shibasaki F (2004) Histone deacetylase 7 associates with hypoxia-inducible factor 1α and increases transcriptional activity. *J Biol Chem* 279(40): 41966–41974.
22. Geng H, et al. (2012) HDAC4 protein regulates HIF1α protein lysine acetylation and cancer cell response to hypoxia. *J Biol Chem* 286:38095–38102.
23. Dioum EM, et al. (2009) Regulation of hypoxia-inducible factor 2α signaling by the stress-responsive deacetylase sirtuin 1. *Science* 324(5932):1289–1293.
24. Lim JH, et al. (2010) Sirtuin 1 modulates cellular responses to hypoxia by deacetylating hypoxia-inducible factor 1α. *Mol Cell* 38(6):864–878.
25. Mimura I, et al. (2012) Dynamic change of chromatin conformation in response to hypoxia enhances the expression of GLUT3 (SLC2A3) by cooperative interaction of hypoxia-inducible factor 1 and KDM3A. *Mol Cell Biol* 32(15):3018–3032.
26. Lee JS, et al. (2011) Hypoxia-induced methylation of a pontin chromatin remodeling factor. *Proc Natl Acad Sci USA* 108(33):13510–13515.
27. Lee JS, et al. (2010) Negative regulation of hypoxic responses via induced Reptin methylation. *Mol Cell* 39(1):71–85.
28. Semenza GL (2010) Defining the role of hypoxia-inducible factor 1 in cancer biology and therapeutics. *Oncogene* 29(5):625–634.
29. Onnis B, Rapisarda A, Melillo G (2009) Development of HIF-1 inhibitors for cancer therapy. *J Cell Mol Med* 13(9A):2780–2786.
30. Wong CC, et al. (2011) Hypoxia-inducible factor 1 is a master regulator of breast cancer metastatic niche formation. *Proc Natl Acad Sci USA* 108(39):16369–16374.
31. Wong CC, et al. (2012) Inhibitors of hypoxia-inducible factor 1 block breast cancer metastatic niche formation and lung metastasis. *J Mol Med (Berl)* 90(7):803–815.
32. Erler JT, et al. (2009) Hypoxia-induced lysyl oxidase is a critical mediator of bone marrow cell recruitment to form the premetastatic niche. *Cancer Cell* 15(1):35–44.
33. Zhang H, et al. (2012) HIF-1-dependent expression of angiopoietin-like 4 and L1CAM mediates vascular metastasis of hypoxic breast cancer cells to the lungs. *Oncogene* 31 (14):1757–1770.
34. Pollard PJ, et al. (2008) Regulation of Jumonji-domain-containing histone demethylases by hypoxia-inducible factor (HIF)-1α. *Biochem J* 416(3):387–394.
35. Cloos PA, et al. (2006) The putative oncogene GASC1 demethylates tri- and dimethylated lysine 9 on histone H3. *Nature* 442(7100):307–311.
36. Whetstine JR, et al. (2006) Reversal of histone lysine trimethylation by the JMJD2 family of histone demethylases. *Cell* 125(3):467–481.
37. Wissmann M, et al. (2007) Cooperative demethylation by JMJD2C and LSD1 promotes androgen receptor-dependent gene expression. *Nat Cell Biol* 9(3):347–353.
38. Wu J, et al. (2012) Identification and functional analysis of 9p24 amplified genes in human breast cancer. *Oncogene* 31(3):333–341.
39. Rui L, et al. (2010) Cooperative epigenetic modulation by cancer amplicon genes. *Cancer Cell* 18(6):590–605.
40. Liu G, et al. (2009) Genomic amplification and oncogenic properties of the GASC1 histone demethylase gene in breast cancer. *Oncogene* 28(50):4491–4500.
41. Jiang BH, Zheng JZ, Leung SW, Roe R, Semenza GL (1997) Transactivation and inhibitory domains of hypoxia-inducible factor 1α. Modulation of transcriptional activity by oxygen tension. *J Biol Chem* 272(31):19253–19260.
42. Zhao H, et al. (2004) Different gene expression patterns in invasive lobular and ductal carcinomas of the breast. *Mol Biol Cell* 15(6):2523–2536.
43. Finak G, et al. (2008) Stromal gene expression predicts clinical outcome in breast cancer. *Nat Med* 14(5):518–527.
44. Karnoub AE, et al. (2007) Mesenchymal stem cells within tumour stroma promote breast cancer metastasis. *Nature* 449(7162):557–563.
45. Semenza GL (2011) Regulation of metabolism by hypoxia-inducible factor 1. *Cold Spring Harb Symp Quant Biol* 76:347–353.
46. Lunt SY, Vander Heiden MG (2011) Aerobic glycolysis: Meeting the metabolic requirements of cell proliferation. *Annu Rev Cell Dev Biol* 27:441–464.
47. Chiang AC, Massagué J (2008) Molecular basis of metastasis. *N Engl J Med* 359(26): 2814–2823.
48. Porter GJ, et al. (2004) Patterns of metastatic breast carcinoma: influence of tumour histological grade. *Clin Radiol* 59(12):1094–1098.
49. Agger K, Christensen J, Cloos PA, Helin K (2008) The emerging functions of histone demethylases. *Curr Opin Genet Dev* 18(2):159–168.
50. Martin C, Zhang Y (2005) The diverse functions of histone lysine methylation. *Nat Rev Mol Cell Biol* 6(11):838–849.
51. Wagner EJ, Carpenter PB (2012) Understanding the language of Lys36 methylation at histone H3. *Nat Rev Mol Cell Biol* 13(2):115–126.
52. Yang L, et al. (2011) ncRNA- and Pc2 methylation-dependent gene relocation between nuclear structures mediates gene activation programs. *Cell* 147(4):773–788.
53. Vaupel P, Mayer A, Höckel M (2004) Tumor hypoxia and malignant progression. *Methods Enzymol* 381:335–354.
54. Semenza GL (2012) Hypoxia-inducible factors: Mediators of cancer progression and targets for cancer therapy. *Trends Pharmacol Sci* 33(4):207–214.
55. Tan H, Wu S, Wang J, Zhao ZK (2008) The JMJD2 members of histone demethylase revisited. *Mol Biol Rep* 35(4):551–556.
56. Wiederschain D, et al. (2009) Single-vector inducible lentiviral RNAi system for oncology target validation. *Cell Cycle* 8(3):498–504.
57. Luo W, et al. (2011) Pyruvate kinase M2 is a PHD3-stimulated coactivator for hypoxia-inducible factor 1. *Cell* 145(5):732–744.
58. Luo W, et al. (2010) Hsp70 and CHIP selectively mediate ubiquitination and degradation of hypoxia-inducible factor (HIF)-1α but not HIF-2α. *J Biol Chem* 285(6): 3651–3663.